Supporting information for:

Reproducibility of Free Energy Calculations Across Different Molecular Simulation Software

Hannes H. Loeffler,[*,†,⊥] Stefano Bosisio,[‡] Guilherme Duarte Ramos Matos,[¶]

Donghyuk Suh,[§] Benoit Roux,[§] David L. Mobley,[‖] and Julien Michel[‡]

*Science & Technology Facilities Council, Daresbury, Warrington WA4 4AD, United
Kingdom, EaStCHEM School of Chemistry, University of Edinburgh, David Brewster Road,
Edinburgh EH9 3FJ, United Kingdom, Department of Chemistry, University of California,
Irvine, University of Chicago, and Departments of Pharmaceutical Sciences and Chemistry,
University of California, Irvine*

E-mail: Hannes.Loeffler@gmail.com

1   Softcore Functions

We describe here the softcore functions[S1,S2] as implemented in the MD packages AMBER,
CHARMM, Gromacs and SOMD. Both the van der Waals, V_{LJ} (Lennard–Jones potential)

*To whom correspondence should be addressed
†Scientific Computing Department, STFC
‡University of Edinburgh
¶University of California, Irvine
§University of Chicago
‖University of California, Irvine
⊥Current address: Eli Lilly and Company, Erl Wood Manor, Sunninghill Road, Windlesham GU20 6PH,
United Kingdom

and the electrostatic interactions, V_{Coul} (Coulomb potential) as a function of the order parameter λ are given for the disappearing atoms only. For the appearing atoms replace λ with $1 - \lambda$ and *vice versa*. Eq. (1) is the generalized form for all codes while the specific distance dependent functions are outlined in eq. (2) for SOMD, eq. (3) for AMBER, eq. (4) for Gromacs and eq. (5) for CHARMM.

$$V = V_{\text{LJ}} + V_{\text{Coul}} = 4\epsilon_{ij}(1 - \lambda)\left[\left(\frac{\sigma_{ij}}{r_{\text{LJ}}}\right)^{12} - \left(\frac{\sigma_{ij}}{r_{\text{LJ}}}\right)^{6}\right] + (1 - \lambda)^{n}\frac{q_i q_j}{4\pi\varepsilon_0 r_{\text{Coul}}} \tag{1}$$

For SOMD

$$
\begin{aligned}
r_{\text{LJ}} &= (\alpha\sigma_{ij}\lambda + r_{ij}^2)^{\frac{1}{2}} \\
r_{\text{Coul}} &= (\lambda + r_{ij}^2)^{\frac{1}{2}}
\end{aligned}
\tag{2}
$$

For AMBER

$$
\begin{aligned}
r_{\text{LJ}} &= (\alpha\sigma_{ij}^6\lambda + r_{ij}^6)^{\frac{1}{6}} \\
r_{\text{Coul}} &= (\beta\lambda + r_{ij}^p)^{\frac{1}{p}} \\
n &= 1
\end{aligned}
\tag{3}
$$

For Gromacs

$$
\begin{aligned}
r_{\text{LJ}} &= (\alpha\sigma_{ij}^w\lambda^p + r_{ij}^w)^{\frac{1}{w}} \\
p &= 1, 2; w = 6, 48; \\
r_{\text{Coul}} &= r_{\text{LJ}} \\
\alpha_{\text{Coul}} &= 0, \alpha_{\text{LJ}} \\
n &= 1
\end{aligned}
\tag{4}
$$

For CHARMM (PSSP), applied to all "reactant" and all "product" atoms

$$r_{\mathrm{LJ}} = (\alpha\lambda + r_{ij}^2)^{\frac{1}{2}}$$
$$r_{\mathrm{Coul}} = (\beta\lambda + r_{ij}^2)^{\frac{1}{2}} \tag{5}$$
$$n = 1$$

r_{vdW}, r_{Coul} and r_{Coul} are distance dependent functions, ϵ_{ij} and σ_{ij} are the Lennard-Jones parameters, q_i and q_j are the charges and ε_0 is the vacuum permittivity, α and β are the softcore tuning parameters determining the softness of the potential, and r_{ij} the distance between atoms i and j.

The exponent n is only used in the Coulomb softcore funtion of SOMD. Gromacs allows additional exponents for λ ($p = 1$ or 2) and w for the distance dependency with values of either 6 or 48. AMBER allows an exponent p (namelist option SCEEORDER) for the Coulomb softcore. The Coulomb softcore parameter α_{Coul} in Gromacs is the same as for the Lennard–Jones parameter α_{LJ} unless the Coulomb softcore function is requested not to be used and thus $\alpha_{\mathrm{Coul}} = 0$. The CHARMM softcore function (PSSP) is applied to *all* atoms in the perturbed group and not only to dummy atoms as in the other codes. The perturbed group comprises of all atoms that need to be transformed, i.e. any atom that differs in at least one force field parameter in the other end state. "Dummy" atom is used here as a shorthand notation for any atom that appears or disappears during the course of the transformation.

2 Split Protocols

When the AFE (alchemical free energy) simulation is separated (split) into van der Waals and Coulomb steps it must be ensured that charges of vanishing atoms are switched off before the vdW radius is scaled to zero. This is to avoid that other atoms e.g. from solvent come in close contact to a charged atom without the associated excluded volume from the van der Waals term as this could lead to large forces and thus instabilities in the integrator.
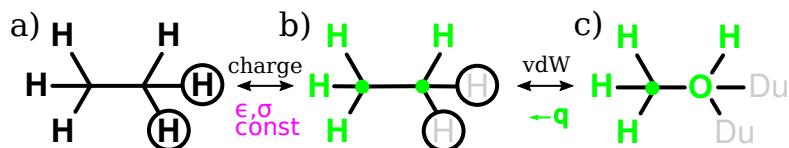
Figure S1: The mutation of ethane into methanol and explicit topologies for three states. a) The two circles denote atoms that have both vdW and Coulomb terms switched on with parameters for the respective hydrogen atom type. b) The two hydrogen atoms have their charges switched to zero (gray symbols in black circle). All other charges are the ones from the methanol end state c (green) to ensures charge neutrality at each step. VdW parameters are constant in the charge transfer step (see annotations in magenta). c) vdW and Coulomb parameters as for methanol while dummy atoms (gray Du) have those parameters all set to zero.

Figure S1 depicts how force field parameters vary for a transformation carried out in the direction of disappearing atoms. The mutation is shown with the charge step first followed by the vdW step but each step can really be run independently. Please note that both charge and vdW step would be simulated at a range of individual λs. Typically the charge transfer is done with linear scaling while the vdW mutation is done with softcores (see above). The transformation is fully symmetrical that is the parameters must be switched on in opposite order if atoms are to be "created". The intermediate state b has the vdW parameters from state a but the charges from state c.

Figure S1 shows how topology files may be created in cases where the MD software does not allow independent λs for electrostatic and vdW mutations. With Gromacs, for instance, the transformation only requires a single topology file with both A and B states (in single topology fashion, see main text) and a single simulation control file with separate λ vectors for charge and vdW transformations. Any intermediate state from Figure S1 is thus created "on–the-fly" i.e. implicitly during the simulation run. With AMBER (up to version 16 as of this writing), however, three explicit topology files (with sander, two with pmemd) and two control files would need to be created. The state b in Figure S1 would be created from state a with the charges from state c. The bonded terms can be combined with either mutation step or run separately. For AMBER the easiest way is to combine vdW with bonded terms because charges are independent of atom types.

Figure S2 illustrates explicit topologies for transformations with both appearing and disappearing atoms in one simulation. The principle is essentially the same as in Figure S1: charges of dummy atoms must be switched off before vdW parameters are set to zero to avoid interactions of "naked" charge sites with other atoms possibly leading to very close contact, large energies and forces, and thus to unstable simulations and/or noisy statistics. However, charge neutrality at every λ step is not supported in most MD codes i.e. the total system charge varies with λ unless the charges of *all* atoms are switched off. Possible strategies would be to explicitly create topology files for each intermediate λ state and distribute the diminished charges from the dummy atoms over to the non–dummy atoms. MD software like CHARMM allows to do this through internal scripting although this would be just as extensive as external scripting the aforementioned strategy.
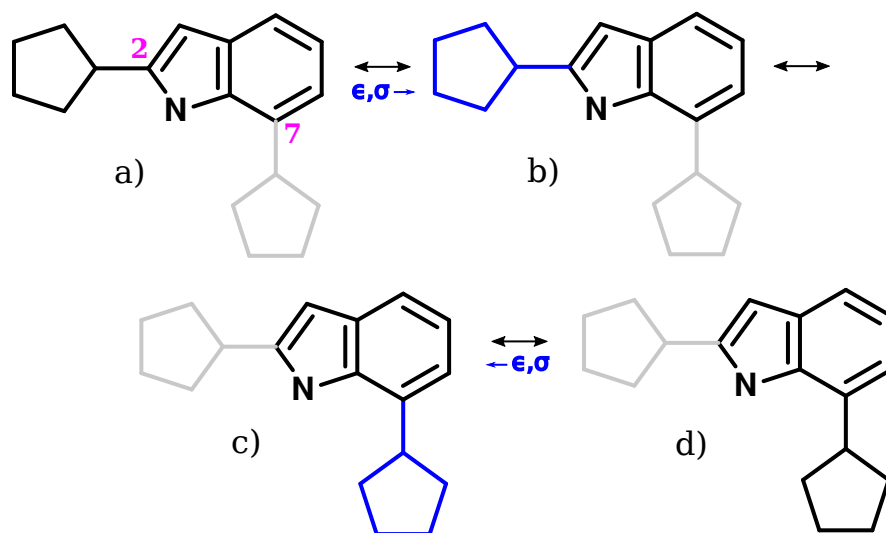

Figure S2: Explicit topologies involved in a mutation with both appearing and disappearing atoms by example of the cyclopentanyl transfer from the 2 position in indole to the 7 position. Blue lines denote atoms which have their charges switched off but with vdW parameters from the left (state b) or right (state c). Gray lines are dummy atoms with Coulomb and vdW parameters all zero. Note, the hydrogen bound to the 2 (state d) and 7 positions (state a) can be directly mutated from the respective carbon atom type without ring breaking.[S3]

With the MD packages tested in this study the number of input files are as follows. With Gromacs this can be done with only two topology and two control files where one charge transfer can be combined with a vdW on/off step. Gromacs' λ vectors only apply

to the perturbed group as a whole and so it is not possible to define a λ vector for only a subset. AMBER requires two such files with sander and three topology/two control files with pmemd for the three steps charge off, vdw on/off and charge on. This is possible because with AMBER a subset of the perturbed group can be chosen to have zero charges (namelist option CRGMASK; but AMBER does not have λ vectors). CHARMM has scripting facilities that let the user manipulate force field parameters of any arbitrary subset of the system such that intermediate states can be defined "on–the-fly" with only one control script and one topology file. The tool FESetup[S4] automates most of these setup steps for all these MD packages.

3 Detailed Results

Table S1: Changes in volumes (in cubic angstrom) for selected perturbations across packages

transformation		AMBER	CHARMM	GROMACS	SOMD
methane	ethane	38±6	24±3	31±3	61±25
ethane	methane	-29±7	-30±4	-28±3	-50±30
ethane	methanol	-33±9	-36±2	-36±5	-66±36
methanol	ethane	38±8	37±3	36±5	46±31
methane	methanol	-5±11	-9±2	-3±5	11±20
methanol	methane	8±10	1±2	4±3	27±16
methane	toluene	93±11	89±3	110±2	120±56
toluene	methane	-106±8	-89±8	-113±3	-145±23
methane	2-methylindole	164±11	64±3	142±3	140±22
2-methylindole	methane	-138±8	-120±7	-139±5	-166±45
methane	neopentane	99±9	90±2	115±4	117±50
neopentane	methane	-105±11	-100±2	-114±4	-68±43

3.1 AMBER

Table S2 compares the split protocol with the unified protocol. The split protocol transforms Coulomb force field parameters separately from the Lennard–Jones and all bonded

parameters. The unified protocol transforms all force field parameters simultaneously and thus invokes both Coulomb and vdW softcore functions.

Table S2: Comparison between split and unified protocol in **AMBER**. The data for the unified protocol highlights inconsistencies in the code in red. ΔG_{sol} has been computed with pmemd. ΔG_{vac} has been computed with sander.

transformation		split protocol			unified protocol		
		ΔG_{sol}	ΔG_{vac}	$\Delta\Delta G$	ΔG_{sol}	ΔG_{vac}	$\Delta\Delta G$
ethane	methane	1.79	1.77	0.02	2.78	2.85	-0.07
methane	ethane	-1.80	-1.80	0.01	-2.87	-2.86	-0.01
methanol	methane	2.74	-3.44	6.19	7.10	0.87	6.23
methane	methanol	-2.75	3.45	-6.19	-7.18	-0.86	-6.32
ethane	methanol	-2.84	3.36	-6.20	-2.25	3.99	-6.25
methanol	ethane	2.83	-3.36	6.19	2.20	-3.99	6.20
toluene	methane	9.22	5.98	3.24	6.09	0.45	5.64
methane	toluene	-9.29	-5.86	-3.42	-6.15	-0.54	-5.61
neopentane[a]	methane	70.16	69.85	0.31	65.76	58.50	7.28
methane[a]	neopentane	-70.17	-69.92	-0.25	-65.82	-58.78	-7.04
neopentane[b]	methane	11.41	11.54	-0.13	4.42	3.48	0.94
methane[b]	neopentane	-11.43	-11.55	0.12	-4.45	-3.49	-0.96
2-methylfuran	methane	14.62	11.53	3.09	2.20	-0.94	3.15
methane	2-methylfuran	-14.60	-11.50	-3.10	-2.22	-0.06	-2.15
2-methylindole	methane	24.25	15.47	8.78	7.11	-4.02	11.13
methane	2-methylindole	-24.31	-15.17	-9.14	-7.13	1.86	-8.97

[a]central mapping.
[b]terminal mapping.

The split protocol produces consistent results in both solution and in vacuum. The values are in line with the free energies obtained with the other MD packages (see main text). Each ΔG is the sum of the charge and vdW plus bonded contributions. The unified protocol on the other hand displays various problems. While the smaller systems with only a few dummy atoms show ΔG and $\Delta\Delta G$ consistent with the split protocol, the larger transformations show, in part, striking differences and even inconsistencies in forward and backward vacuum simulations. It is not clear, however, if the inconsistencies can be attributed to the vacuum transformations only.

Figure S3 shows a problem with end point geometries. This is demonstrated with the

average distance between the carbon atom and the four attached hydrogens atoms in the neopentane to methane case. The methane carbon atom is mapped here to the central atom of neopentane. The distances are recorded for the vdW plus bonded transformation i.e. the charges correspond to the methane end state.
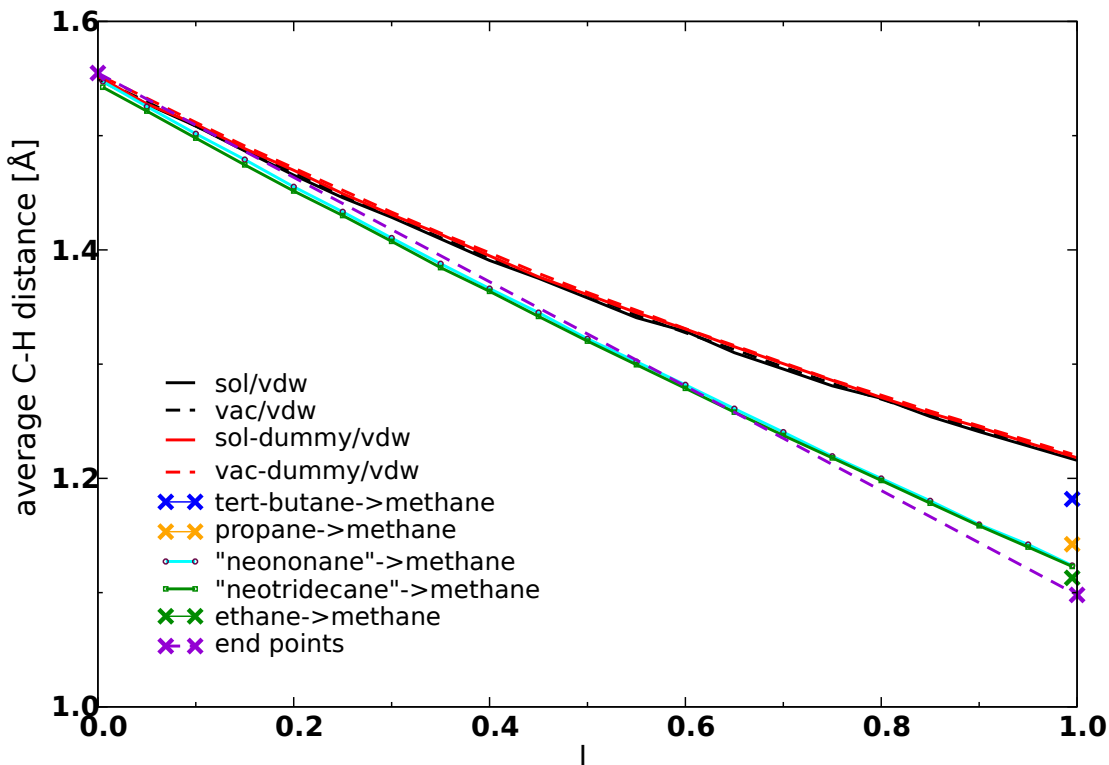

Figure S3: **AMBER** : The average C–H distance shown as a function of λ for the neopentane to methane and related cases. The black and red lines display how the distance changes in solution and the vacuum phase, and with and without explicit dummy atoms. The other test systems are designed to reduce the number of dummy atoms that surround the central carbon atom to show whether "crowding" is the cause of the issue. The crosses denote end points only, in particular the violet crosses represent the non–perturbed end point distances. For details see the text.

The geometrical variation along λ for the data in the main text is shown in the black and red graphs. The initial distance is slightly smaller than what is expected from a C–H

distance for the particular atom types at $\lambda = 0$. The final distance is about $1.23\,\text{Å}$ which is in contrast to the $1.09\,\text{Å}$ of the c3–hc bond of the GAFF force field. The crosses in violet mark the geometries of the "pure" (non–perturbed) end points and are connected with a straight line. The other crosses denote test cases which successively replace the methyls on neopentane with hydrogens. The C–H distance decreases in correlation with the number of the methyl groups i.e. tert-butane, propane, ethane. This seems to suggest that a "crowding" of dummy atoms around a central atom compounds the problem of a too long C–H distance. Neither of these three test cases, however, displays the expected end point distance.

To further test this hypothesis methyl and ethyl groups are added to all terminal methyl groups of neopentane, see cyan and green lines in Figure S3. In both cases the end point distance is about $1.12\,\text{Å}$ with a slightly lower value for the ethyl substitution but which are still too high.

As Gromacs conveniently allows us to use a separate λ for bonded terms we tested this on the neopentane case. After the charges were transformed to the methane end state (dummy atoms have zero charges), the bonded terms were mutated from neopentane to methane while the vdW parameters were kept constant at the neopentane initial state. The observed end distance was about $1.23\,\text{Å}$ which is to be expected given that the symmetrically arranged methyl groups will repel each other and thus not allow to reach the final distance. Only after the final vdW (only) mutation had been carried out, were the final distances of $1.09\,\text{Å}$ reached.

Table S3 summarizes the free energy components for the 2–methylindole to methane case for both forward and backward transformations. The electrostatic contributions display a very small SEM and the averages from both directions agree with each other up to the second digit after the comma. The van der Waals contributions show a higher SEM and the averages from the solution simulations agree well with each other. However, the van der Waals contributions from the vacuum transformation are apart by $0.3\,\text{kcal}\,\text{mol}^{-1}$ (highlighted in red).

Table S3: **AMBER**: Free energy components for 2–methylindole computed from implicit dummy RAFE simulations. The data are averages over three runs.

transformation		$\Delta G_{\mathrm{sol}}^{\mathrm{vdW}}$	SEM	$\Delta G_{\mathrm{vac}}^{\mathrm{vdW}}$	SEM	$\Delta G_{\mathrm{sol}}^{\mathrm{elec}}$	SEM	$\Delta G_{\mathrm{vac}}^{\mathrm{elec}}$	SEM
2-methylindole	methane	4.83	0.02	3.48	0.01	19.41	0.01	11.99	0.01
methane	2-methyindole	-4.90	0.02	-3.18	0.01	-19.41	0.01	-11.90	0.01

In sum, this indicates a problem of the RAFE code in AMBER. Whether that is a bug or a conceptual issue with the particular implementation can not be explained at the moment.

Table S4 summarizes the free energies obtained from forward and backward simulations of the cyclopentanyl transfer from position 2 to position 7 on indole and *vice versa*. Results from three different protocols are shown: 1) implicit dummy atoms and partial re/discharge of the 5–ring only; 2) implicit dummy atoms and full re/discharge of all atoms; 3) explicit dummy atoms and partial re/discharge. The free energies from the implicit dummy simulations agree very well with each other while the explicit dummy atom results are about $0.2\,\mathrm{kcal\,mol^{-1}}$ higher and forward and backward simulations have a larger hystersis of $0.1\,\mathrm{kcal\,mol^{-1}}$.

Table S4: **AMBER**: Free energies of hydration for the 2–cyclopentanylindole to 7–cyclopentanylindole case with three different protocols. The data are averages over three runs.

transformation		ΔG_{sol}	SEM	ΔG_{vac}	SEM	$\Delta\Delta G_{\mathrm{hydr}}$	SEM
implicit, partial							
2–cyclopentanylindole	7–cyclopentanylindole	4.19	0.03	3.83	0.01	0.36	0.03
7–cyclopentanylindole	2–cyclopentanylindole	-4.30	0.04	-3.96	0.01	-0.33	0.04
implicit, full							
2–cyclopentanylindole	7–cyclopentanylindole	4.28	0.06	3.92	0.02	0.36	0.07
7–cyclopentanylindole	2–cyclopentanylindole	-4.41	0.03	-4.10	0.01	-0.32	0.03
explicit, partial							
2–cyclopentanylindole	7–cyclopentanylindole	4.14	0.04	3.51	0.04	0.63	0.06
7–cyclopentanylindole	2–cyclopentanylindole	-4.25	0.03	-3.76	0.01	-0.50	0.03

3.2 SOMD

As discussed in the main tex, the presend SOMD calculations used a shifted atom-based Barker-Watts reaction field cutoff to handle electrostatic interactions in solutions and a Coulomb laws without cutoffs to handle electrostatic interactions in vacuum. This leads to an inconsistent description of the intramolecular electrostatic interactions of the solute in the solvated and vacuum phases. To maintain a consistent description of intramolecular energetics across vacuum and water legs, a free energy correction term ΔG_{c} was evaluated as detailed in Ref.[S5] The ΔG_{c} term was obtained via post-processing of the end state trajectories of each water phase simulation, using the Zwanzig relationship:[S6]

$$\Delta G_{\mathrm{c}} = -\beta^{-1} \ln \langle \exp \left[-\beta (U_{\mathrm{ic,nc}}(\mathbf{r}) - U_{\mathrm{ic,sim}}(\mathbf{r})) \right] \rangle_{\mathrm{sim}} \tag{6}$$

where $U_{\mathrm{ic,nc}}(\mathbf{r})$ is the solute intramolecular electrostatic-no cutoff potential that depends on the coordinates $\mathbf{r}$ of the solute and is given by Coulomb's law computed without cutoffs. $U_{\mathrm{ic,sim}}(\mathbf{r})$ is the intramolecular electrostatic potential term as computed in the simulation with the shifted atom-based Barker-Watts Reaction Field cutoff.

Figure S4 compare relative free energy of hydration $\Delta\Delta G$ with relative $\Delta\Delta G$ estimations from absolute free energy calculations for all the transformation of the dataset.
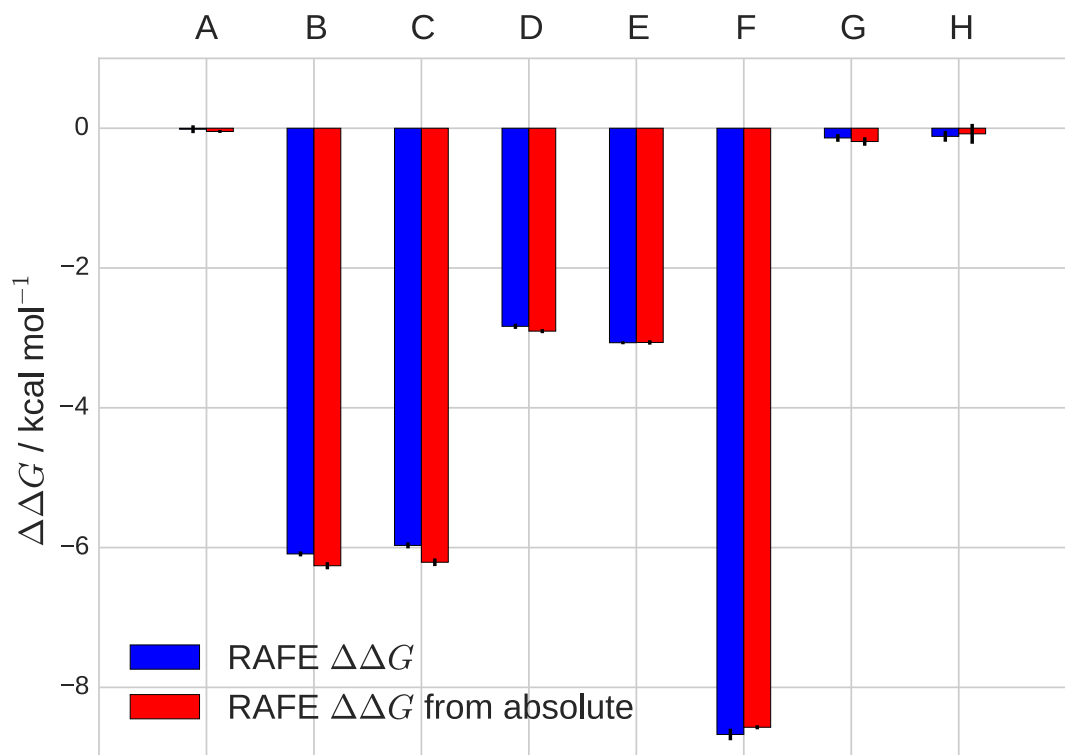
Figure S4: **SOMD**: Relative free energy of hydration $\Delta\Delta G$, computed with RAFE calculations, compared with $\Delta\Delta G$ derived from absolute free energy calculations for A: methane to ethane, B: ethane to methanol, C: methane to methanol, D: methane to 2-methylfuran, E: methane to toluene, F: methane to 2-methylindole, G: methane to neopentane, H: 2-cyclopentanylindole to 7-cyclopentanylindole.

Table S5 shows relative free energy of hydration $\Delta\Delta G$ compared to $\Delta\Delta G$ values extracted from absolute free energy calculations, depicted in Fig S4.

Initially, SOMD RAFE protocols used all bonds constraint algorithm. In this way all the solute bonds are constrained, which results in a systematic offset for each RAFE predictions, compared to the RAFE from absolute free energy calculations. Figure S5 shows the discrepancy between RAFE computed with all bond constraints and RAFE from absolute free energy calculations.

Table S5: **SOMD**: Final relative free energy of hydration $\Delta\Delta G$ estimations and standard error SEM with Sire/SOMD unperturbed hydrogen bonds protocol, RAFE, compared with relative free energy of hydration computed from absolute free energy simulations, RAFE-absolute. Signs in backward transformation are reverted for better comparison.

| transformation		RAFE		RAFE-absolute	
		$\Delta\Delta G$	SEM	$\Delta\Delta G$	SEM
ethane	methane	-0.01	0.05	0.04	0.02
methane	ethane	-0.04	0.02	0.04	0.02
methanol	methane	5.99	0.05	6.21	0.05
methane	methanol	5.96	0.04	6.21	0.05
ethane	methanol	-6.09	0.03	-6.26	0.05
methanol	ethane	-6.09	0.02	-6.26	0.05
toluene	methane	2.89	0.03	3.06	0.03
methane	toluene	3.06	0.02	3.06	0.03
neopentane[a]	methane	-0.20	0.054	-0.19	0.06
methane[a]	neopentane	-0.13	0.055	-0.190	0.060
neopentane[b]	methane	-0.11	0.01	-0.19	0.06
methane[b]	neopentane	-0.10	0.06	-0.19	0.06
2-methylfuran	methane	2.92	0.05	2.90	0.03
methane	2-methyfuran	2.83	0.03	2.90	0.03
2-methylindole	methane	8.64	0.06	8.57	0.03
methane	2-methylindole	8.67	0.08	8.57	0.03
2–cyclopentanylindole	7–cyclopentanylindole	0.11	0.077	0.08	0.14
7–cyclopentanylindole	2–cyclopentanylindole	0.01	0.081	0.08	0.14

[a]central mapping.
[b]terminal mapping.
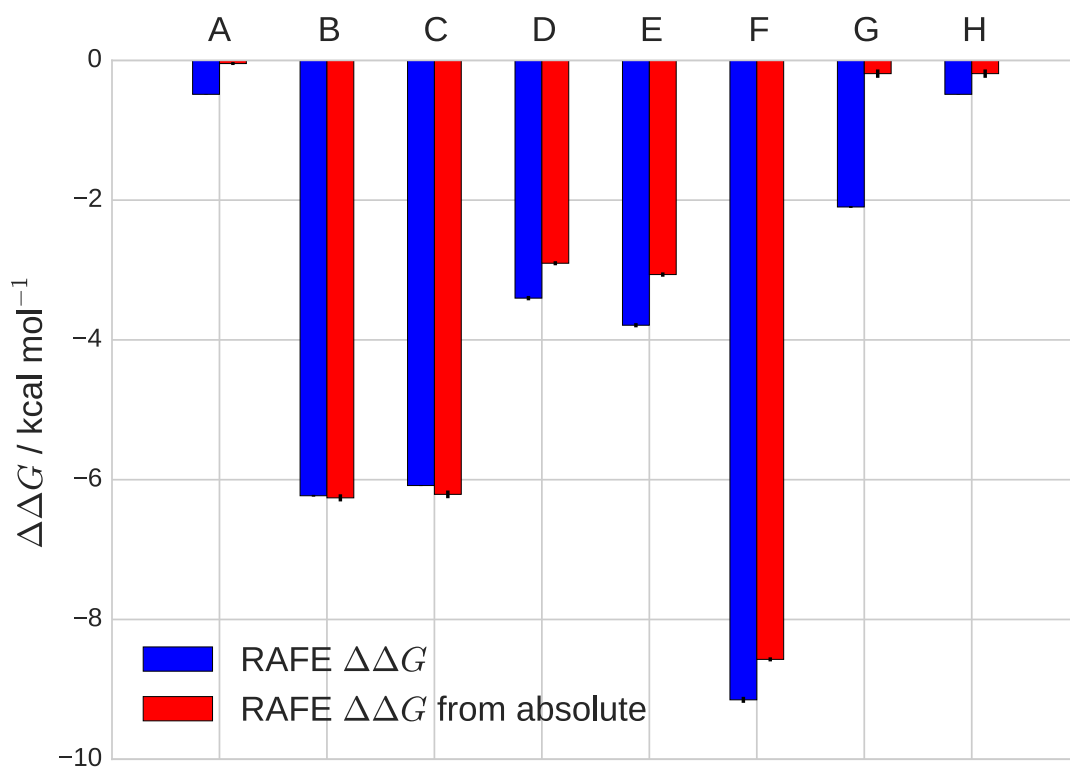
Figure S5: **SOMD**: Comparison between RAFE of hydration computed with all bond constraints and RAFE computed from absolute free energy calculations

Finally, figure S6 and table S6 compare relative free energy of hydration $\Delta\Delta G$ estimated with RAFE using all bonds constraints, no constraints and unperturbed hydrogen bond constraints.

Table S6: **SOMD**: Relative free energy of hydration $\Delta\Delta G$ computed with all bond constraints, *All bonds*, no constraints, *None*, and unperturbed hydrogen bond constraint, *unpert H bonds*

transformation		All bonds		None		unpert H bonds	
		$\Delta\Delta G$	SEM	$\Delta\Delta G$	SEM	$\Delta\Delta G$	SEM
ethane	methane	-0.48	0.01	-0.18	0.04	-0.01	0.05
methane	ethane	-0.49	0.01	-0.01	0.02	-0.04	0.02
methanol	methane	6.06	0.01	6.49	0.01	5.99	0.05
methane	methanol	6.08	0.01	6.15	0.01	5.96	0.04
ethane	methanol	-6.22	0.01	-6.14	0.03	-6.09	0.03
methanol	ethane	-6.23	0.01	-6.09	0.01	-6.09	0.02
toluene	methane	3.73	0.27	3.09	0.06	2.89	0.09
methane	toluene	3.79	0.03	3.07	0.06	3.06	0.02
neopentane[a]	methane	-2.09	0.01	-0.14	0.14	-0.20	0.05
methane[a]	neopentane	-2.04	0.01	-0.018	0.06	-0.13	0.05
neopentane[b]	methane	-0.48	0.01	-0.14	0.06	-0.11	0.01
methane[b]	neopentane	-0.59	0.02	-0.14	0.060	-0.10	0.06
2-methylfuran	methane	3.38	0.02	2.81	0.03	2.92	0.05
methane	2-methyfuran	3.40	0.03	2.89	0.06	2.83	0.03
2-methylindole	methane	9.29	0.06	8.72	0.05	8.63	0.06
methane	2-methylindole	9.10	0.04	8.61	0.04	8.67	0.08

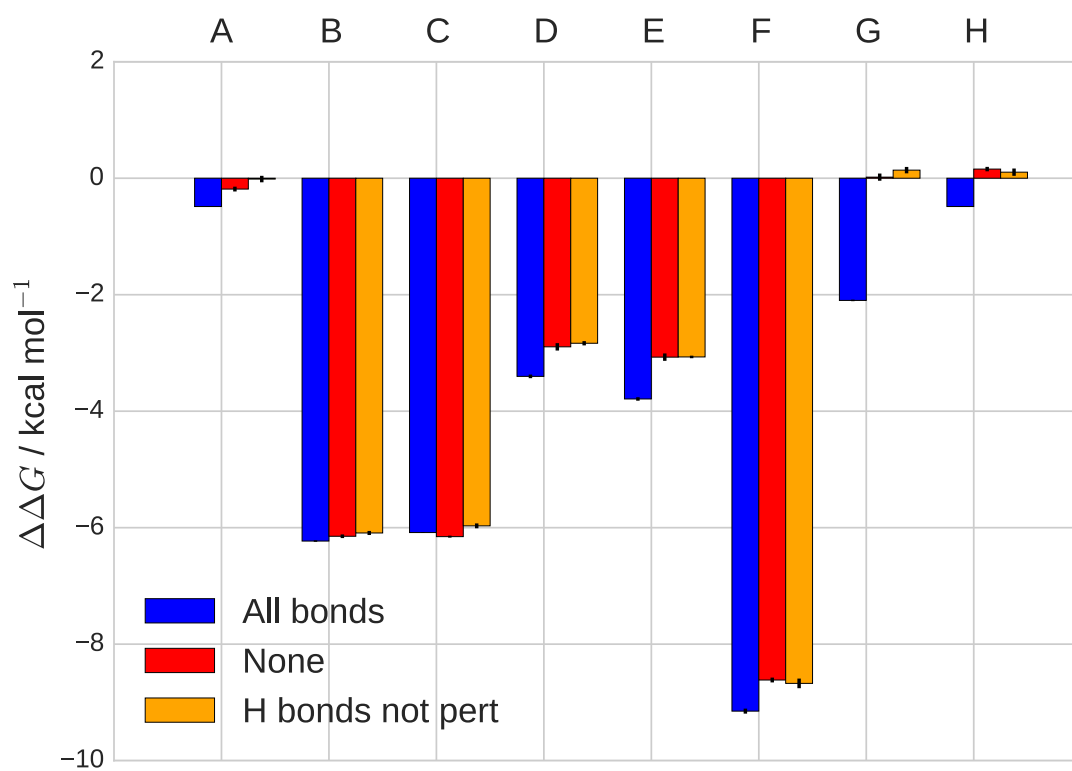[a]central mapping.
[b]terminal mapping.

Figure S6: **SOMD**: Comparison between RAFE of hydration computed with all bond constraints, no constraints and unperturbed hydrogen bonds constraint

3.3 GROMACS

Table S7 compares RAFE results subject to the use of Coulomb softcore potentials. In principle, the use of softcore functions is redundant in the split protocol because charges are changed while van der Waals parameters are fully tuned to the transformation's final state parameters. SEM values tend to be larger when they are used.

Table S7: **GROMACS**: $\Delta\Delta G_{hydr}$ results in different scenarios with or without Coulomb softcore potentials, in kcal $\cdot$ mol^{-1}.

Transformations		without Coulomb softcore RF $\Delta\Delta G$	PME $\Delta\Delta G$	with Coulomb softcore RF $\Delta\Delta G$	PME $\Delta\Delta G$	absolute RF $\Delta\Delta G$	PME $\Delta\Delta G$
ethane	methane	-0.02 ± 0.01	-0.03 ± 0.02	-0.03 ± 0.04	-0.02 ± 0.04	-0.06 ± 0.01	-0.04 ± 0.01
methane	ethane	-0.01 ± 0.02	-0.02 ± 0.01	-0.01 ± 0.04	-0.02 ± 0.04		
methanol	methane	6.16 ± 0.01	6.20 ± 0.01	7.32 ± 0.03	7.42 ± 0.04	5.77 ± 0.01	5.95 ± 0.01
methane	methanol	6.17 ± 0.01	6.20 ± 0.01	7.14 ± 0.03	7.21 ± 0.03		
ethane	methanol	-6.12 ± 0.01	-6.19 ± 0.01	-6.15 ± 0.02	-6.21 ± 0.02	-5.83 ± 0.01	-5.98 ± 0.01
methanol	ethane	-6.12 ± 0.01	-6.19 ± 0.01	-6.15 ± 0.02	-6.21 ± 0.02		
toluene	methane	3.22 ± 0.01	3.211 ± 0.010	3.22 ± 0.04	3.21 ± 0.04	2.97 ± 0.01	3.16 ± 0.01
methane	toluene	3.25 ± 0.01	3.20 ± 0.01	3.27 ± 0.04	3.22 ± 0.04		
neopentane[a]	methane	-0.10 ± 0.01	-0.15 ± 0.02	-0.13 ± 0.08	-0.13 ± 0.08	-0.18 ± 0.01	-0.14 ± 0.01
methane[a]	neopentane	-0.11 ± 0.02	-0.16 ± 0.05	-0.12 ± 0.08	-0.15 ± 0.08		
neopentane[b]	methane	-0.12 ± 0.01	-0.13 ± 0.01	-0.10 ± 0.04	-0.13 ± 0.04		
methane[b]	neopentane2	-0.10 ± 0.03	-0.18 ± 0.03	-0.08 ± 0.06	0.15 ± 0.06		
2-methylfuran	methane	2.97 ± 0.01	2.93 ± 0.05	3.07 ± 0.03	3.02 ± 0.04	2.87 ± 0.01	2.95 ± 0.01
methane	2-methylfuran	3.00 ± 0.01	2.96 ± 0.01	3.08 ± 0.03	3.02 ± 0.04		
2-methylindole	methane	8.71 ± 0.02	8.73 ± 0.03	8.79 ± 0.04	8.82 ± 0.05	8.44 ± 0.02	8.79 ± 0.02
methane	2-methylindole	8.73 ± 0.03	8.74 ± 0.01	8.79 ± 0.05	8.81 ± 0.06		
2-cyclopentanylindole	7-cyclopentanylindole	-0.07 ± 0.02	-0.03 ± 0.03	-0.12 ± 0.03	-0.14 ± 0.05	-0.02 ± 0.05	0.02 ± 0.02
7-cyclopentanylindole	2-cyclopentanylindole	-0.12 ± 0.06	-0.20 ± 0.04	1.20 ± 0.20^c	1.50 ± 0.10^c		

[a]central mapping
[b]terminal mapping
[c] inverted sign

The effect of the Coulomb softcore potential can be seen in Figure S7.
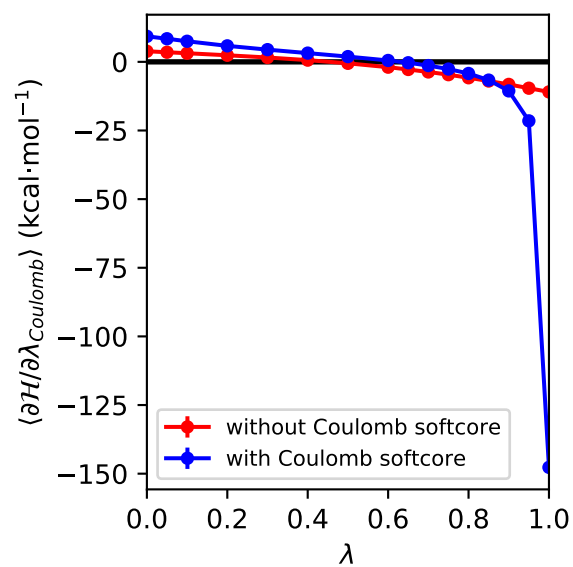
Figure S7: **GROMACS**: $\langle \partial \mathcal{H} / \partial \lambda \rangle$ plot for the change in electrostatic terms in methane $\rightarrow$ methanol.

3.4 CHARMM

Figure S8 shows the effect of turning long range corrections (LRC) on/off as function of the cut–off values on the absolute solvation free energy of methane. The switching function starts $2\,\text{Å}$ before the cut-off value. The figure shows that cutoff values greater than $10\,\text{Å}$ give consistent results, if the LRC has been disabled. The bottom graph shows the relative solvation free energy of 2–methylindole to methane from direct RAFE and from AAFEs of methane and 2–methylindole with LRC on/off. This shows that the protocols will be inconsistent by ca. $0.8\ kcal.mol^{-1}$ if the LRC is not disabled. By post-processing LRC, RAFE result was more comparable to the results from other MD packages.
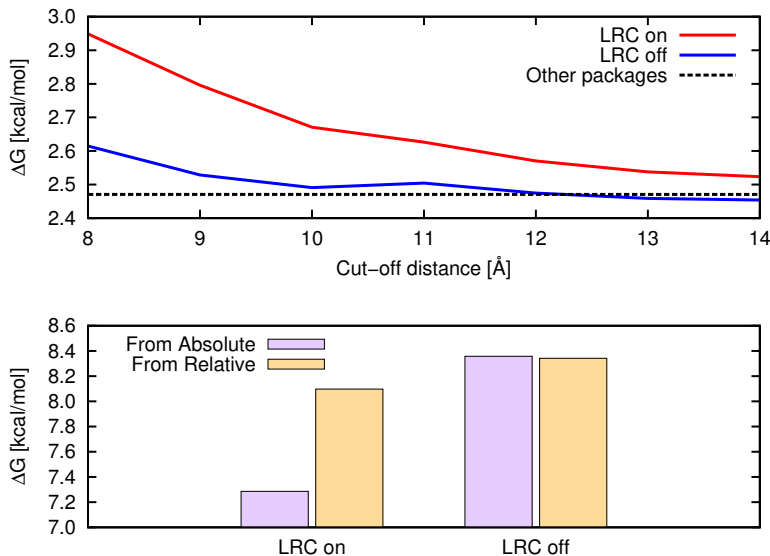

Figure S8: **CHARMM**: (top) Absolute solvation free energy of methane as a function of different cut–off values and presence or absence of a Long Range Correction term. (bottom) Relative solvation free energy between 2–methylindole and methane from relative or absolute alchemical free energy protocols and with/out a LRC term.

References

(S1) Beutler, T. C.; Mark, A. E.; van Schaik, R. C.; Gerber, P. R.; van Gunsteren, W. F. *Chemical Physics Letters* **1994**, *222*, 529–539.

(S2) Zacharias, M.; Straatsma, T. P.; McCammon, J. A. *The Journal of Chemical Physics* **1994**, *100*, 9025–9031.

(S3) Liu, S.; Wang, L.; Mobley, D. L. *Journal of Chemical Information and Modeling* **2015**, *55*, 727–735, PMID: 25835054.

(S4) Loeffler, H. H.; Michel, J.; Woods, C. *Journal of Chemical Information and Modeling* **2015**, *55*, 2485–2490.

(S5) Bosisio, S.; Mey, A. S. J. S.; Michel, J. *Journal of Computer-Aided Molecular Design* **2016**, *30*, 1101–1114.

(S6) Zwanzig, R. *The Journal of Chemical Physics* **1954**, *22*, 1420–1426.